

A STUDY FOR THE EFFECT OF CORRELATION BETWEEN WINDS AND WAVES ON THE CAPSIZING PROBABILITY UNDER DEAD SHIP CONDITION

Yoshitaka Ogawa, National Maritime Research Institute, Japan ogawa@nmri.go.jp

ABSTRACT

A database of world wind and wave is constructed by the data composed of the hindcasting data, which can provide both winds and wave data simultaneously. Having compared with the existing wave data, the characteristics of the present hindcasting data is discussed. The correlation between winds and waves is also discussed. Through calculations of the capsizing probability by means of the piece-wise linear approach, the effect of the correlation between winds and waves on the capsizing probability is examined. Finally, the best correlation between winds and waves for the calculation of the capsizing probability under dead ship condition is discussed.

Keywords: *new generation intact stability criteria, dead ship condition, capsizing probability, correlation between wind and wave*

1. INTRODUCTION

It is well known that a ship suffers beam winds and waves when all her operational means such as propeller thrust and rudder control are lost. Therefore, it is important to assess the capsizing probability under dead ship condition properly and to provide the adequate requirements for ensuring safety.

In particular, since the International Maritime Organization (IMO) started to develop the new-generation intact stability criteria for three major capsizing modes, which contains the stability under dead ship conditions, with performance based approaches, the construction of a reliable methodology for estimating a capsizing probability is an urgent issue for the proper provision of the safety.

With regard to the capsizing probability under dead ship conditions, some practical methods for estimating the capsizing probability, e.g. piece wise linear method (Belenky, 1994, Paroka, et al., 2006), have been proposed and validated through the calculation of the probability in short term sea

states (e.g. Ogawa, 2008). It is expected that those method can be utilized within the framework of new-generation intact stability criteria.

In the meanwhile, for the provision of the criteria with performance-based approaches, the capsizing probability in the long-term sea states should be assessed. It is well known that wind has much effect on the capsizing probability under dead ship conditions. It implies that the capsizing probability in the long-term sea states should be conducted taking into account of the correlation between wind and wave. However, there are few studies for the correlation between winds and waves and for its effect on the capsizing probability.

Based on the background, first, a database of world winds and waves is constructed by means of the hindcasting data, which can provide both winds and waves data synchronized in space and time. Having compared with the existing wave data, the characteristics of the present hindcasting data is discussed. The correlation between wind and wave is also discussed.



Second, the capsizing probability is calculated by means of two kinds of correlation between winds and waves. One is the statistical correlation based on the present hindcasting data. The other is that wind is fully correlated wave height based on the WMO's (World Meteorological Organization) reference data. Through those calculations of the capsizing probability, the effect of the correlation between winds and waves on the capsizing probability is examined.

Finally, the correlation between winds and waves for the application to the direct calculation of capsizing probability for the present purpose is discussed.

2. WORLD WIND AND WAVE DATA

2.1 Source Data of Winds and Waves

For the examination of correlation between winds and waves, it is preferable that wind data synchronize with wave data in space and time. Based on this background, the wave and wind statistics are composed by the wave hindcasting data, which can have applicability for the present purpose. The present hindcasting data are computed by means of the third generation wave hindcasting model of Global Climate by Japan Weather Association (JWA3G model). Grid point value (GPV) of sea winds, provided by the Meteorological Agency of Japan, is used as an input of this model. Significant wave height, wave period and peak direction of waves, mean wind speed and wind direction every 6 hours are computed. These are composed by lattice of 2.5 degree interval (all area from 70 degrees of North latitude to 70 degrees of South latitude). In the present study, data of the 10-year span from January 1997 to December 2006 are used.

The third generation wave hindcasting models basically adopt not conservative methods such as SMB method or PNJ method but the spectral method, which is the

mainstream of the ocean waves forecasting/hindcasting model. A spectral method is the method computes individual growth and attenuation of each component wave. Prior to the application, the validity of numerical computation of JWA3G model was verified (Japan Weather Association, 1993) through the numerical simulation in accordance with the SWAMP (Sea Wave Modeling Project) method (The SWAMP group, 1985). The SWAMP method is justified the validity in 1979 through the project for constructing a verification method of the numerical computation of ocean wave. Almost existing numerical models were verified its validity through numerical simulation of the SWAMP method.

Computed waves were verified through the comparison with measured wave data by means of a buoy and an artificial satellite. It was clarified that error of wave height is 0.9 m from 0.5 m and bias error is about 0.5 m from 0.05 m. It was verified that the correlation coefficient with buoy data is 0.9 from 0.65. It was also clarified that the accuracy of computed wave height was quite improved than that of previous numerical model (Japan Weather Association, 1993).

However, it is to below significant wave height of 10 m that the accuracy was verified through the comparison with buoy data. It is well known that wave exceeds 10 m is rarely observed by the buoy. This means that verification of accuracy of over 10 m wave height is not necessarily sufficient. Moreover, the accuracy of measured high wave by means of buoy should be clarified because it is considered that the structural characteristics of mooring of buoy may have effects on measuring of high wave.

2.2 Characteristic of Wind and Wave Data

Figures 1 to 3 show the contour of average of significant wave height. Figures 4 to 6 show the contour of average wind speed. Area of zero wave height and wind speed corresponds to the land. It is found that wave on Southern Hemisphere become higher in spring and summer season and waves on Northern Hemisphere become higher in autumn and winter season. Moreover, it is found that wave height in North Pacific, North Atlantic Ocean and South Indian Ocean are higher compared with other sea area. It is also found that spatial distribution of wave height is consistent with that of wind speed. It is clarified that these findings are consistent with existing findings.

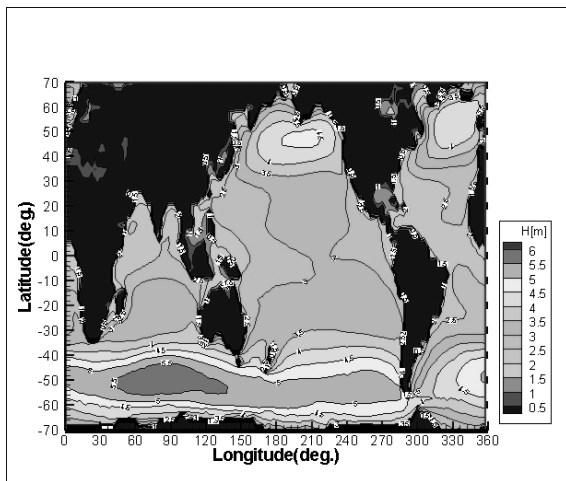


Figure 1. Contour of average of significant wave height (annual).

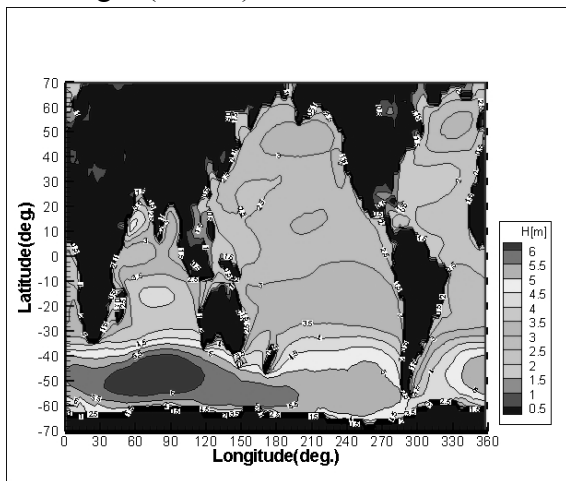


Figure 2. Contour of average of significant wave height (summer: June - August).

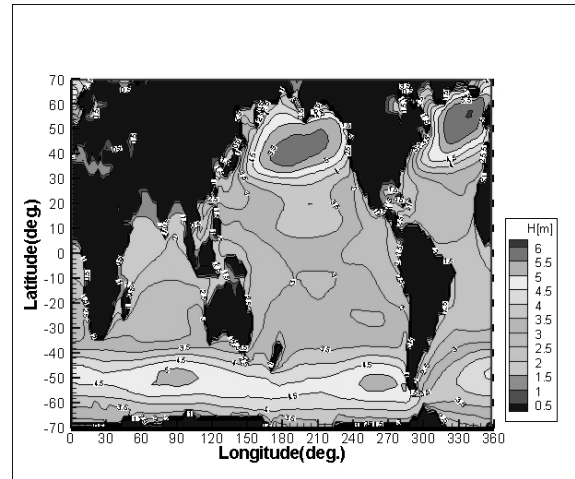


Figure 3. Contour of average of wave height (winter: December - February).

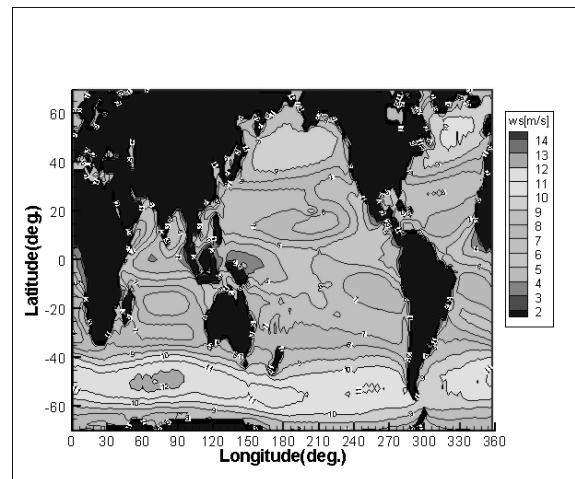


Figure 4. Contour of mean wind speed (annual).

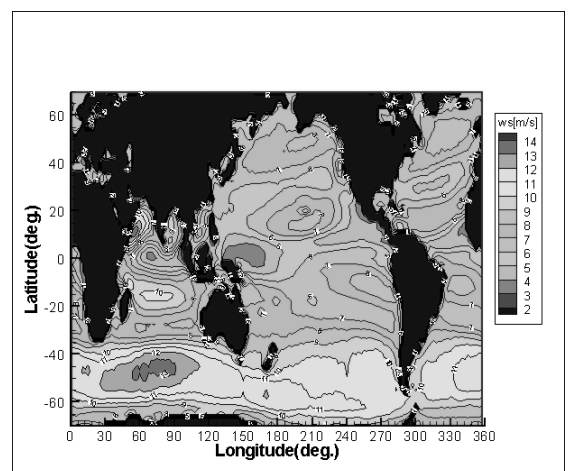


Figure 5. Contour of mean wind speed (summer: June - August).

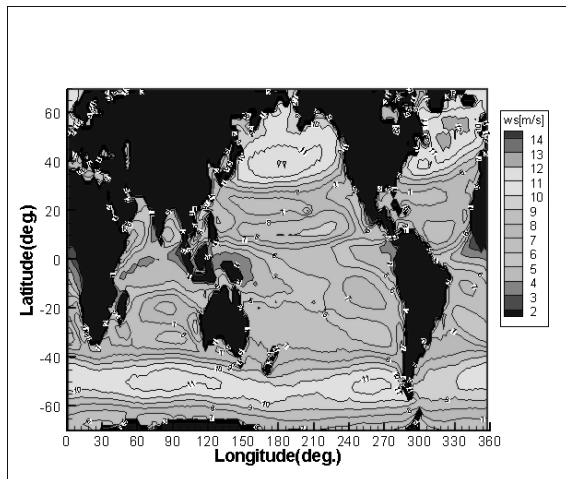


Figure 6. Contour of mean wind speed (winter: December - February).

However, it is found that average of significant wave height is about higher than that of existing wave statistics (e.g. Global Wave Statistics (GWS: British Maritime Technology Limited, 1985)) 1.0m particularly in North Pacific, North Atlantic Ocean and South Indian Ocean. It was clarified that wave height is higher than that of buoy 10% (Japan Weather Association, 1993). It is clarified that these findings are same as the results concluded through the verification of JWA3G. Figure 7 and Figure 8 show the highest 1/1000 value of significant wave height and wind speed. It is also found that these waves in North Pacific, North Atlantic Ocean and South Indian Ocean are higher than those of existing wave statistics (e.g. GWS). These differences are remarkable in areas whose wave height is relatively higher.

Through the verification of JWA3G model, it has been clarified that attenuation of low frequency wave is weaker than that of high frequency wave due to the characteristics of model of energy dispersion mechanism. Therefore, it is considered that swell of longer period has much effect on the wave height in severer sea conditions such as North Pacific, North Atlantic Ocean and South Indian Ocean.

3. CORRELATION BETWEEN WINDS AND WAVES

For the present purpose for calculation of the capsizing probability, the statistical characteristics are also important because not only the magnitude of wave height but also the probability of occurrence of wave height has effects on the capsizing probability. The probability of occurrence of the JWA3G wave data, which are verified physically, is examined through the comparison with the probability of existing wave data.

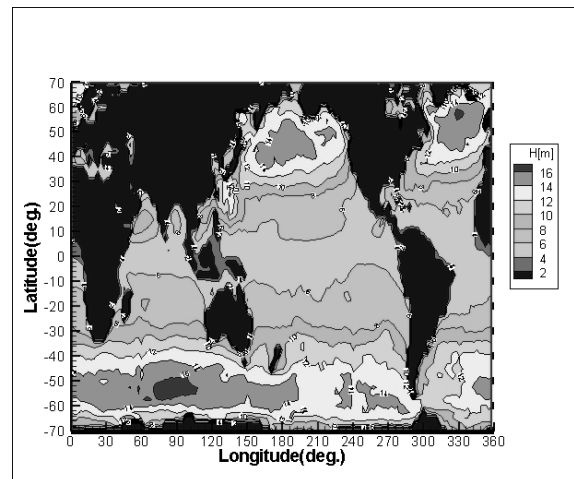


Figure 7. Contour of highest 1/1000 value of wave height (annual).

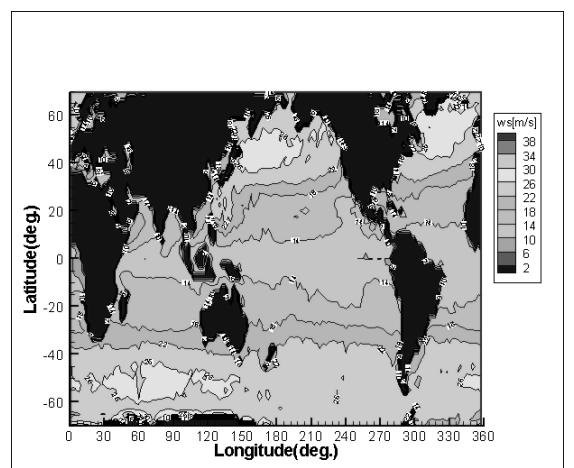


Figure 8. Contour of highest 1/1000 value of wind speed (annual).

Figure 9 shows the definition of sea area in the present analysis. Figure 10 shows examples of comparison of probability of occurrence as a function of significant wave height. Wave in North Atlantic Ocean (A4 in Figure 9) and Indian Ocean (N2 in Figure 9) are compared with the probability based on the Global Wave Statistics (GWS: British Maritime Technology Limited, 1985). It is clarified that probability from around Indian Ocean becomes much similar to those of GWS. In the meanwhile, probability of high wave in Pacific Ocean and Atlantic Ocean becomes much higher than those of GWS. This is consistent with the findings shown from Figure 1 to Figure 8.

Correlation between wind speed and wave is examined based on the scatter diagram of wave height–wind speed and wave period–wind speed. Maximum wave height and wave period at each wind speed in those scatter diagram are related to each wind speed. Correlation in North Pacific, North Atlantic Ocean and South Indian Ocean are shown in Figure 11 and 12. The correlations based on the Beaufort chart are also shown in Figure 11 and 12. In this chart, wave height is defined based on the WMO’s reference data and wave period is defined based on the Pierson-Moskowitz equation.

Although the JWA3G model adopted the spectral method in computation, it is found that the relation between wave height and wind speed in each sea area becomes similar. It is also found that correlation of JWA3G is similar to that of Beaufort chart qualitatively. In the meanwhile, wave height of JWA3G is higher than that of Beaufort chart 2.0 m.

It is clarified that there are significant discrepancies of statistical characteristics of high wave from existing ones although the validity of numerical model of JWA3G was verified. For the further consideration, correlation of wind speed and wave height is examined from the viewpoint of fetch and duration of wind. Figure 13 shows the Chart for estimation of wind waves. This is a chart to

estimate wave height and period by the wind speed, fetch and duration. Relation between wind speed and wave in accordance with Beaufort chart are shown in Figure 13 as circles. Fetch and duration assumed in the Beaufort chart are estimated by wind speed, wave height and wave period. It is found that fetch assumed in Beaufort chart is correspond to 30 hours from 16 hours, which are put between two dotted vertical diagonal lines in Figure 13. In accordance with those fetches, it is found that wind speed of 30 m/s generates 14 m from 10 m wave height and wind speed of 40 m/s generates 22 m from 16 m wave height. It is possible that about wave of 20 m height are generated under the strong wind with long duration. In addition, in the JWA3G model, wind keeps same speed and same direction at one point during 6 hours, which is a time interval of hindcasting. In the real condition, it is possible that wind fluctuate with a certain range. Therefore, it is supposed that those differences of wind can cause a difference of high wave although computation of JWA3G model operates adequately.

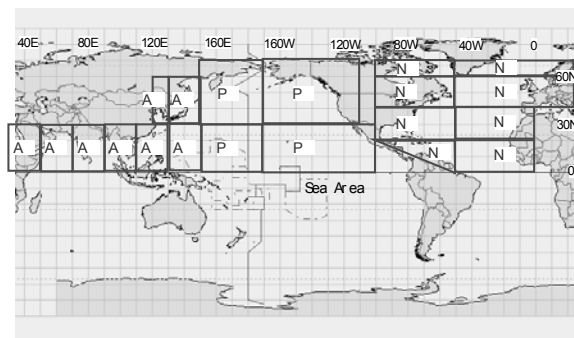


Figure 9. The sea area as the object of the present study.

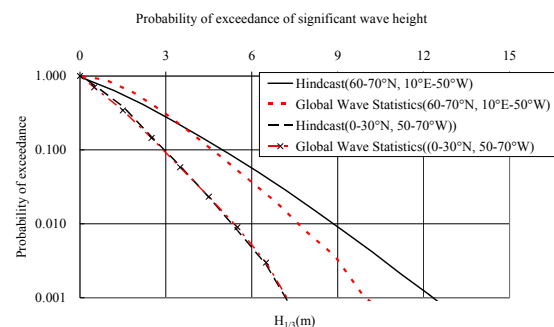


Figure 10. Probability of exceedance of wave height.

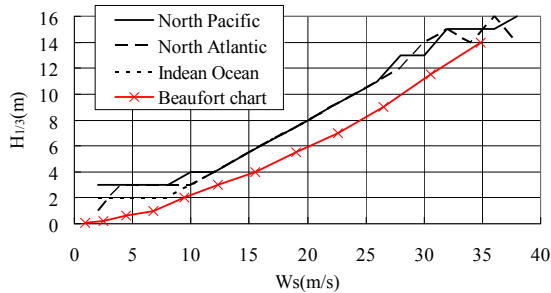


Figure 11. Relation between wind speed and significant wave height.

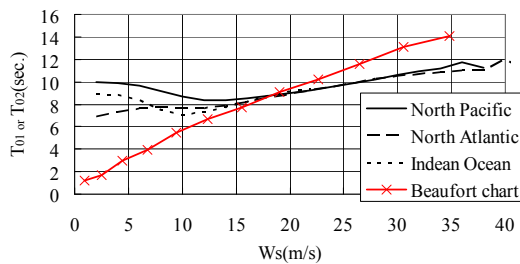


Figure 12. Relation between wind speed and wave period.

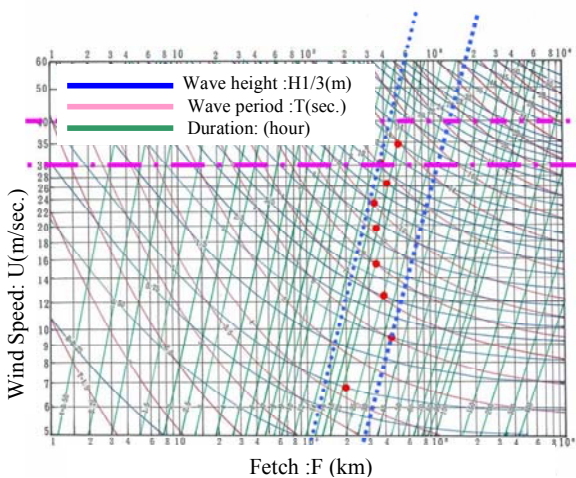


Figure 13. Chart for estimation of wind waves.

4. CALCULATION OF CAPSIZING PROBABILITY

4.1 Capsizing Probability by means of The Piece-wise Linear Approach

In the present study, a capsizing probability within a stationary sea state is calculated using

the piece-wise linear approach, which was developed by Belenky (Belenky, 1993, 1994) and sophisticated by Paroka (Paroka et al., 2006). This method can calculate probability analytically by means of the piece-wise linear approximation of righting arm, shown in Figure 14. This is partly because it rigorously takes account of nonlinear restoring moment and its efficient calculation load enables us to obtain annual capsizing probability by integrating many combinations of wave height and wave period in long-term wave statistics.

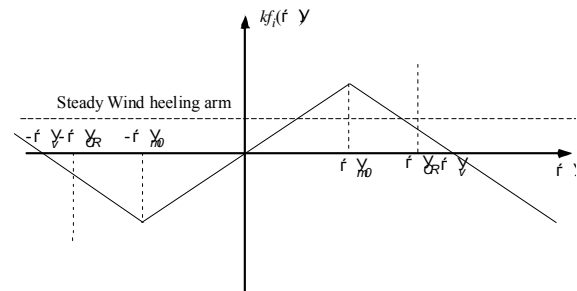


Figure 14. Piece-wise linear approximation of righting arm.

The capsizing probability here is calculated with the following nonlinear and uncoupled equation of rolling angle of a ship under a stochastic wave excitation and wind moment. Usually the ship motion in beam sea is modelled with equations of coupled motions in sway and roll with wave radiation forces and diffraction forces. Watanabe (1938), however, proposed an one-degree of freedom equation of roll angle, ϕ , as follows

$$(I_{xx} + A_{44})\ddot{\phi} + B_{44}\dot{\phi} + WGZ(\phi) = M_{wind}(t) + M_{wave}(t) \quad (1)$$

where I_{xx} is momentum of inertia of the ship, A_{44} is the hydrodynamic coefficient of added inertia, W is the ship displacement, B_{44} is the hydrodynamic coefficient of roll damping, $GZ(\phi)$ is the righting arm. $M_{wind}(t)$ is the wind induced moment consisting of the steady and fluctuating wind moment and $M_{wave}(t)$ is the wave exciting moment based on the Froude-Krylov assumption. This is because the roll

diffraction moment and roll radiation moment due to sway can cancel out when the wavelength is sufficiently longer than the ship breadth. (Tasai, 1969)

The uncoupled equation of the absolute roll motion (1) can be rewritten by dividing by the virtual moment of inertia as follows:

$$\ddot{\phi} + 2\alpha\dot{\phi} + \omega_0^2 kf_i(\phi) = \omega_0^2 (m_{wind}(t) + m_{wave}(t)) \quad (2)$$

where $kf_i(\phi) = GZ(\phi)/GM$, α : roll damping coefficient, ω_0 : the natural roll frequency and $kf_1(\phi)$: the non-dimensional righting arm, $m_{wind}(t)$: the wind induced moment consisting of the steady and fluctuating wind moment and $m_{wave}(t)$: the wave exciting moment based on the Froude-Krylov assumption.

As shown in Fig. 14, the restoring moment coefficient in equation (2) is approximated with continuous piece-wised lines in leeward and windward conditions as follows:

$$kf_i(\phi) = \begin{cases} kf_0\phi & 0 < \phi < \phi_{m0} \text{ range1} \\ kf_1(\phi_v - \phi) & \phi_{m0} < \phi \text{ range2} \end{cases} \quad (3)$$

and

$$kf_i(\phi) = \begin{cases} kf_0\phi & -\phi_{m0} < \phi < 0 \text{ range1} \\ kf_1(-\phi_v - \phi) & \phi < -\phi_{m0} \text{ range2} \end{cases} \quad (4)$$

Here, kf_0 and kf_1 are the slope of the range 1 and range 2, respectively. ϕ_{m0} and $-\phi_{m0}$ are the border between the range 1 and the range 2 in leeward and windward, respectively. Effects of dividing methods of the righting arm curve into piece-wise lines and the case using the relative roll angle can be found in Paroka, et al. (2006).

Since Equation (2) is linear within each range, it can be analytically solved without any problems. The border condition, however, should be satisfied. Therefore, capsizing occurs

when the roll angle up-crosses, ϕ_{m0} , or down-crosses, $-\phi_{m0}$, and then the absolute value of roll angle increases further. Therefore, capsizing probability can be calculated as the product of the out-crossing probability in the range 1 and the conditional probability of divergence of the absolute value of roll angle in the range 2. The probability that a ship capsizes when the duration, T , passes in stationary waves can be described as follows, (Umeda, et al., 2004)

$$P(H_{1/3}, T_{01}, W_s, T) = P_l P_T(\phi > \phi_{m0} \text{ or } \phi < -\phi_{m0}) P_A(A > 0; \phi > \phi_{m0}) + P_w P_T(\phi > \phi_{m0} \text{ or } \phi < -\phi_{m0}) P_A(A < 0; \phi < -\phi_{m0}) \quad (5)$$

where $H_{1/3}$: the significant wave height, T_{01} : the mean wave period, W_s : the mean wind velocity and T : duration. P_l and P_w denote the probability of up-crossing toward leeward and that of down-crossing toward windward. Under the assumption of Poisson process, P_T indicates the probability of at least one up-crossing or down-crossing at the border between the first and second range, ϕ_{m0} or $-\phi_{m0}$. P_A is the probability of diverging behaviour of absolute value of the roll angle in the second range including the angle of vanishing stability. These can be determined as follows:

$$P_T(\phi > \phi_{m0} \text{ or } \phi < -\phi_{m0}) = 1 - \exp(-(u_l + u_w)T) \quad (6)$$

$$P_l = \frac{u_l}{u_l + u_w} \quad (7)$$

$$P_w = \frac{u_w}{u_l + u_w}$$



$$P_A(A > 0; \phi > \phi_{m0}) = \int_0^{\infty} f(A) dA$$

$$P_A(A < 0; \phi < -\phi_{m0}) = \int_{-\infty}^0 f(A) dA \quad (8)$$

where u_l and u_w denote the expected number of up-crossing and down-crossing, respectively. $f(A)$ denotes the probability density function of the coefficient A , which is a function of three random variables, namely the initial angular velocity of roll motion, $\dot{\phi}_l$, the initial forced roll, p_l , and the initial forced angular velocity, \dot{p}_l , in the second range. The probability density function of the A coefficient can be determined from a joint probability density function of these three random variables, which can be calculated by means of the three-dimensional Gaussian probability density (Price and Bishop, 1974).

For evaluating risk of capsizing, it is necessary to calculate annual capsizing probability with sea state statistics of operational water area. The formula of the annual capsizing probability, P_{an} , can be found in Iskandar et al. (2000) as follows:

$$P_{an} = 1 - (1 - P^*(T))^{365 \times 24 \times 3600 / T} \quad (9)$$

where

$$P^*(T) = \int_0^{\infty} \int_0^{\infty} f(H_{1/3}, T_{01}) \cdot P(H_{1/3}, T_{01}, W_s, T) dH_{1/3} dT_{01} \quad (10)$$

4.2 The Effect of Correlation between Winds and Waves on Capsizing Probability

For the examination of the effect of probabilistic distribution of wave and wind data, the capsizing probability of the RO-PAX

ferry ($L_{pp}=170$ m, Natural roll period: $T_r=17.9$ s) is calculated. This ship was used to evaluate the weather criterion in the IMO Intact Stability code (Ishida, 2006).

In the numerical calculation, the roll damping coefficients, the wind heeling moment and the aerodynamic coefficient of this ship are given by the experiments respectively (Ishida, 2006). The effective wave slope coefficient is calculated by the strip method taking account of the coupling sway motion. Duration of sea state is defined as an hour. The wind velocity is assumed to be constant and time-dependent variation of wind velocity is ignored. The 1964 ISSC spectrum is used for the modelling of the ocean waves.

Figure 15 shows the righting arm (GZ) curves of the present Ro-PAX ferry. The limiting KG, which is governed by the weather criterion, is used as a loading condition. The approximated line of the righting arm curve, of which GM, the area under the GZ curve and the angle of vanishing stability are not changed, is also shown in Figure 15.

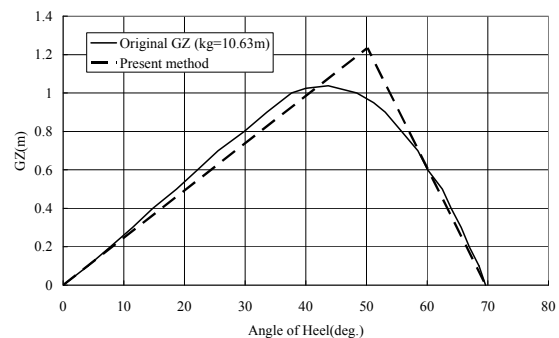


Figure 15. Piece-wise linear approximation of righting arm of RO-PAX ferry.

Figure 16 shows the long-term capsizing probability within one year based on two kinds of scatter diagram of winds and waves in the North Atlantic. One is the scatter diagram of wave height, wave period and wind speed, which is derived from the JWA3G data. The other is the scatter diagram of IACS recommendation No.34 (IACS, 2001). This is the diagram of wave height and wave period, which was derived from the GWS data in

North Atlantic Ocean. Wind speed is determined from wave height based on the WMO's reference data.

The capsizing probability by means of JWA3G data is the long-term prediction. This is not a function of wind speed. Therefore, the probability at the highest wind speed in Figure 16 corresponds to a long-term probability. However, to check the change of capsizing probability within the calculation, the change of capsizing probability as wind speed increases is shown in Figure 16. It is found that the capsizing probability based on the JWA3G data is higher than that based on the GWS. It is clarified that the higher probability of high wave shown in Figure 10 and the longer wave period of slow wind shown in Figure 12 have effects on the difference of capsizing probability.

For the comparison, the short-term capsizing probability is calculated assuming that wave is fully correlated with wind speed in accordance with the Beaufort chart. The long-term probability converted from that short-term capsizing probability is also shown in Figure 16. It is found that the capsizing probability at lower wind speed based on the JWA3G data is higher than the probability in accordance with the Beaufort chart. It is clarified that the higher wave shown in Figure 11 and the longer wave period at slow wind shown in Figure 12 have effects on the difference of capsizing probability.

In addition, taking the correlation coefficient with buoy data in North Atlantic was 0.764 (Japan Weather Association, 1993) and the correlation between winds and waves shown in Figure 11 into account, 20% of wave height in the scatter diagram derived by the JWA3G data are revised downward. The long-term capsizing probability based on this scatter diagram is also shown in Figure 16. It is found that the capsizing probability becomes similar to that based on the GWS. It is clarified that the probability of high wave has much effect on the capsizing probability.

For the application of direct calculation, it is preferable that the method of calculation is robust and inputs for calculation should not include uncertainties. Based on findings of the present study, it is clarified that wave of JWA3G data has the case to be higher and longer than that of existing data although computation of JWA3G model operates adequately. It is also clarified that those uncertainties of wave has much effect affect on the capsizing probability. In the meanwhile, it is verified that the correlation between wind and wave are as qualitatively same as that of WMO's reference data. Furthermore, it is found that capsizing probability with the reduction of wave height becomes consistent with the probability assuming the correlation based on the WMO's reference data. Based on these findings, it is concluded that utilization of hindcasting data for the capsizing probability is premature at the current stage. It is practical to calculate the capsizing probability assuming the correlation between wind and wave based on the WMO's reference data.

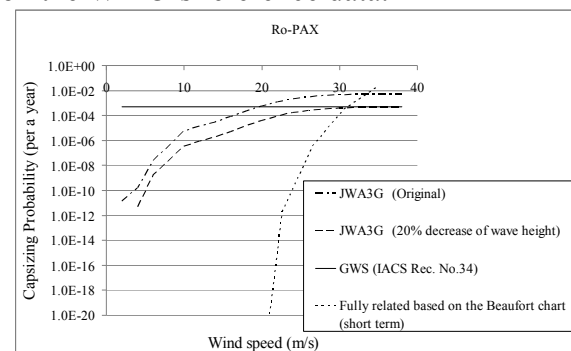


Figure 16. The effect of wave data on annual capsizing probability of the Ro-PAX ferry under dead ship condition.

5. CONCLUSIONS

For the application of direct calculation of the capsizing probability under dead ship condition, the correlation between winds and waves is examined by means of the hindcasting data. Conclusions are as follows:

- 1). The correlation between winds and waves in hindcasting data is as qualitatively same as that in accordance with the WMO's



reference data and the Pierson-Moskowitz equation.

- 2). Waves of the present hindcasting data tend to be higher wave than those of existing data (e.g. GWS). These differences are remarkable in North Pacific and North Atlantic Ocean due to the characteristics of model of energy dispersion mechanism.
- 3). The capsizing probability with the reduction of wave height of hindcasting data is consistent with the probability assuming the correlation based on the WMO's reference data.
- 4). The capsizing probability assuming the correlation between wind and wave based on the WMO's reference data is practical for the direct calculation of the capsizing probability at the current state of the art of wave data.

6. ACKNOWLEDGMENTS

A part of the present study was carried out in cooperation with the Japan Ship Technology Research Association through the part of the Japanese project for the stability safety that is supported by the Nippon Foundation.

7. REFERENCES

- Belenky, V.L., 1993, "A Capsizing Probability Computation Method", *Journal of Ship Research*, Vol. 37, pp.200-207.
- Belenky, V.L. 1994, "Piece-wise Linear Methods for the Probabilistic Stability Assessment for Ship in a Seaway", *Proceedings of the 5th International Conference on Stability of Ship and Ocean Vehicles*, Melbourne, 5, pp.13-30.
- British Maritime Technology Limited, 1985, "Global Wave Statistics".
- Ishida, S. Taguchi, H. and Sawada, Y. 2006. "Evaluation of the Weather Criterion by Experiments and its Effect to the De-sign of a RoPax ferry", *Proc. of 9th International Conference on Stability of Ships and Ocean Vehicles*.
- Ogawa, Y., Umeda, N., Paroka, D., Taguchi, H., Ishida, S., Matsuda, A., Hashimoto, H. and Bulian G., 2008, "Prediction method for capsizing under dead ship condition and obtained safety level – Final report of SCAPE committee (Part 4) -", *Conference Proceedings of the Sixth OSAKA Colloquium (OC2008) on Seakeeping and Stability of ships*.
- Paroka, D., Ohkura, Y. and Umeda, N., 2006, "Analytical Prediction of Capsizing Probability of a Ship in Beam Wind and Waves", *Journal of Ship Research*, Vol. 50, No.2, pp. 187-195
- Price, W. G. and Bishop, R.E.D., 1974, "Probabilistic Theory of Ship Dynamics", London: Chapman and Hall Ltd.
- The SWAMP group, 1985, "Ocean wave modelling", Plenum Press.
- Tasai, F. and Takagi, M., 1969, "Theory and calculation method for response in regular waves", *Seakeeping Symposium (in Japanese)*, The Society of Naval Architects of Japan.
- IACS, 2001, "Standard Wave Data", Unified Requirement No.34.
- Iskandar, B. H., N. Umeda and M. Hamamoto, 2000, "Capsizing Probability of an Indonesian RoRo Passenger Ship in Irregular Beam Seas", *Journal of the Society of Naval Architects of Japan*, 188, pp.183-189.
- Japan Weather Association, 1993, "Research and development of the ocean-waves prediction model and waves information service system by means of a spherical-surface coordinate system".
- Umeda, N., Ohkura, Y., Urano, S. and Hori, M., 2004, "Some Remarks on Theoretical Modelling of Intact Stability", *Proceedings of the 7th International Ship Stability Workshop*, Shanghai, pp. 85-91.